UNIVERSITY OF COPENHAGEN
FACULTY OF SCIENCE

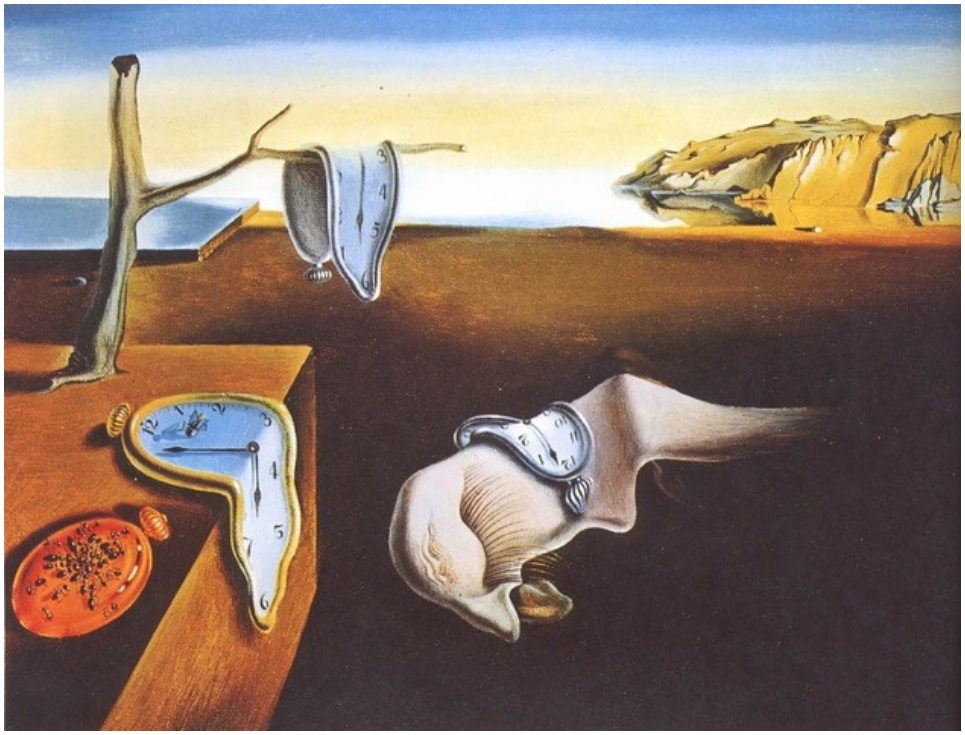

Master's degree thesis

Marc Plana Caballero

Mesoscopic chemical clocks in coupled compartments

Supervised by Mogens H. Jensen and Mathias Heltberg

Handed in: September 2020

Contents

Part I
Introduction

What is a 'good' clock? How to build one? Keeping track of the time is fundamental to all living beings. Mechanisms marking the rhythms of life rely on an accurate control of timing in organisms at all levels of complexity, from intracellular mechanisms such as gene expression and cell division control in prokaryotes [1], up to regulation of entire multicellular beings, as in daily sleep-wake cycles in mammals or other circadian clocks [4][5]; and operate at time scales that are orders of magnitude apart, with the heart beating at a pace of the order of a second and menstruation happening once a month. Understanding the underlying molecular mechanisms as well as the operating principles of biological clocks has, therefore, theoretical and practical implications in sensibly any field of biology and medicine. Indeed, the study of biological clocks has been a major field of research for some decades, with even a Nobel prize awarded to Hall, Rosbash and Young for their "discoveries of molecular mechanisms controlling the circadian rhythm" [2].

But how do living beings keep track of the time? The core mechanism of biological clocks is usually credited to a set of chemical reactions containing some negative feedback mechanism [6]. Many simple models of chemical reactions that undergo cyclic dynamics have been devised, many of them as simplified versions of the so-called Belousov-Zhabotinsky reaction [16]. These models have served as simple frameworks in order to develop analytical and experimental tools for the understanding of chemical oscillations. As simple as they are, some insight can be gained using these simplistic models.

However, only keeping track of the time is usually insufficient for many given purposes. For example, the pacemaker cells in our hearts not only keep a constant rhythm, but do so synchronously. Wherever a biological clock is present, synchronicity most probably is as well. It is, thus, a major concept in the field. The theoretical landmark to study the synchronization of oscillating units has been the Kuramoto model [7]. In this model, a population of oscillators is considered, where each of them exhibits a natural frequency for self-sustained oscillations which are assumed to be the result of a limit-cycle solution to some governing dynamical system. The oscillators are then weakly coupled to one another, by introducing some coupling functions modulated by a coupling strength. A phase transition occurs at a critical value of the coupling strength, where the population of oscillators shifts from a totally asynchronous phase to a state where a group of oscillators lock to a common phase [11].

There is one effect that could be considered as competing with synchronization: noise. There are multiple sources of noise with very distinct natures; we will focus on the noise associated to dealing with a finite number of interacting agents. In chemical reactions, for example, it is not possible to follow the trajectory of every molecule, so we focus on statistical properties such as reaction rates. The stochasticity stems from these statistical considerations. Regarding biological

clocks, it is known that stochasticity causes the period of the oscillations to fluctuate. The interplay between noise and biochemical oscillations has been explored both theoretically [8] and experimentally [9].

Now we are in a position to finally describe what is the aim of this work. On the one hand, the finiteness of a chemical oscillatory system causes fluctuations in the period of the oscillations. On the other hand, synchronization between oscillators causes them to entrain to one another. How do these effects interact? Is it possible to improve the 'robustness' of a limit cycle to stochastic fluctuations by means of synchronization?

To explore this question, we abstractly divide a reaction container with some fixed and finite volume in two separate compartments, and then consider some sort of transport between these as a way of synchronizing both. We seek to understand whether or not is possible to retrieve a better oscillator from this coupling -here 'better' meaning with a less fluctuating period, more robust-. The possibilities here are vast, so we limit to some few configurations and present some arguments on why we do not see an improvement in the period distribution, or rather why we do see an improvement in one of the cases. In the latter, we argue that this mechanism may not be of biological relevance.

At least one alternative mechanism has been devised as a viable way of obtaining sustained oscillations. Suppose there is a system of reactions that can be modelled, in the deterministic limit, by a set of equations that approach a steady state value asymptotically in time. We now want to consider systems that approach the fixed point in an oscillatory manner, i.e., systems that spiral-in hyperbolically when they get close enough to the fixed point. If one onsiders the finite-population version of such systems, where noise is present due to the stochastic nature of the individual reactions taking place, noise acts as a destabilizing force, kicking the system out of its otherwise stationary state. In certain conditions, the natural spiralling around this limiting state has been found to be sufficient in order to define maintained oscillations [12]. As it will be discussed in the following pages, these oscillations cannot be understood or described by means of the Kuramoto model. We also discuss the possible effect of coupling in this particular case.

Part II
Preliminaries

The aim of this section is to introduce the raw ingredients that will be used throughout the present work. These are described with more or less detail, with the focus set on getting a general picture of every one of them and why they are important or useful for our study.

A toy model of a chemical clock: the Brusselator system

In looking for examples of oscillating chemical reactions, the most popular and well-known of them all is the Belousov-Zhabotinsky reaction (BZR). This reaction was first discovered by the soviet chemist Boris Belousov in 1951: he observed that a mix of potassium bromate, cerium(IV), sulfate, malonic-acid and citric acid in dilute sulphuric acid caused the colour of the solution to change from yellow to colourless and back to yellow for an extended period of time.

Different abstract models were developed thereafter, not with the intention of exactly reproducing the dynamics of the BZ reaction, but rather to get simpler reaction networks where sustained oscillations arouse, in order to study them from an analytical standpoint. One of these simplistic models is the one we will be using all throughout this work: the Brusselator model. [16]

The following set of four reactions define the chemical network of the Brusselator model:

$$\begin{aligned} \emptyset &\xrightarrow{1} X \\ 2X + Y &\xrightarrow{c} 3X \\ X &\xrightarrow{b} Y \\ X &\xrightarrow{1} \emptyset \end{aligned}$$

The rates of the first and last reactions can be (and are) set to unity without loss of generality, if units of time and concentrations are defined appropriately. If we consider these reactions in a well-mixed container and an infinite population of molecules, the deterministic dynamics are described by the set of non-linear ODEs:

$$\begin{aligned} \dot{x} &= 1 + cx^2y - bx - x \\ \dot{y} &= -cx^2y + bx \end{aligned} \tag{1}$$

Linear-stability analysis

There is only one fixed point for the system, $(x^*, y^*) = (1, b/c)$. Its local stability is determined by the eigenvalues of the Jacobian at the equilibrium point, namely:

$$\mu = \begin{pmatrix} 2cxy - b - 1 & cx^2 \\ -2cxy + b & -cx^2 \end{pmatrix}_{x^*,y^*} = \begin{pmatrix} b-1 & c \\ -b & -c \end{pmatrix} \tag{2}$$

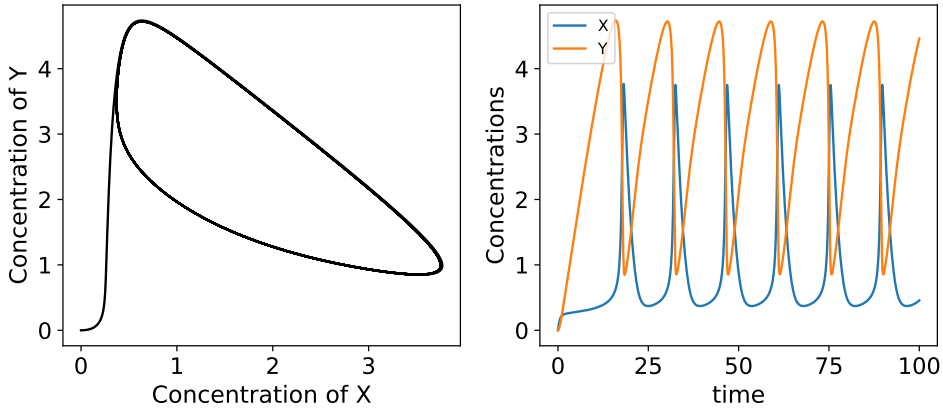

Figure 1: Sample trajectories for a Brusselator above the Hopf bifurcation. Left: a trajectory in phase-space. Right: Time evolution for each variable.

The sign of the eigenvalues can be discussed using the determinant and trace. The fixed point is linearly stable if λ_1, λ_2 have negative real parts. This is equivalent (using the characteristic equation) to $\Delta > 0$ and $\tau < 0$, these being the determinant and trace of A^*, respectively. We have:

$$\Delta = c; \quad \tau = b - 1 - c \tag{3}$$

The determinant is positive for any value of the rates b, c. However, the sign of the trace defines two disjoint regions in parameter space: for $b > 1 + c$ it is positive, whereas for $b < 1 + c$ it is negative. So, we have found a bifurcation at the borderline value $b_C = 1 + c$. For values $b < b_C$ the fixed point is a sink, for values $b > b_C$ both eigenvalues have positive real parts and hence the fixed point is a source.

Existance of a limit cycle: the Poincaré-Bendixon theorem

What happens to the trajectories when the fixed point is repulsive? There are no other fixed-points in the system, so they either go to infinity in some fashion, or approach some bounded region. In planar systems such as this one, the Poincaré-Bendixon theorem establishes that trajectories have a very limited amount of possibilities: they either approach a fixed point, diverge to infinity, or approach a closed orbit. We can try to find a trapping region: a closed, connected set in phase space such that the vector field $(\dot{x}, \dot{y})$ points inwards at all boundaries -implying that a trajectory starting at the region does never leave the region, hence discarting the possibility that it goes to infinity- and with no fixed points in its interior. Then, all trajectories are 'trapped' inside this region, so according to the theorem they must asymptotically approach a closed orbit (or be a closed orbit) [10], since this is the only remaining possibility.

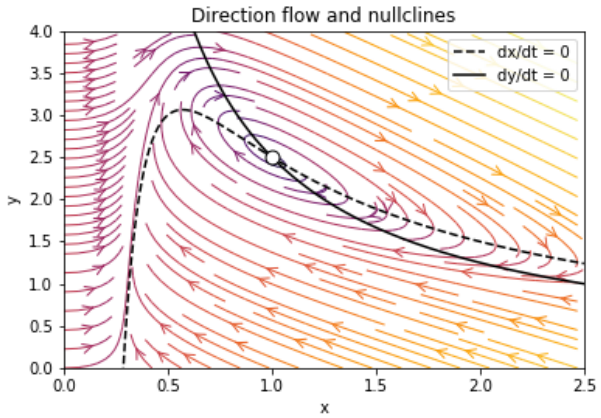

Figure 2: Nullclines $y_1(x)$ and $y_2(x)$ for $b = 2.5$ and $c = 1$. The fixed point (repulsive) is indicated by an empty small circe at the crossover of both nullclines. The lines give an idea of the direction flow in phase space, with a color gradient representing the local modulus of $(\dot{x}, \dot{y})$.

A trapping region can be constructed in the following way. Let us first have a look at the nullclines $\dot{x} = f(x, y) = 0$ and $\dot{y} = g(x, y) = 0$. Writing them in the form $y(x)$ they are:

$$\begin{aligned} y_1(x) &= \frac{(b+1)x - 1}{cx^2} \\ y_2(x) &= \frac{b}{cx} \end{aligned} \tag{4}$$

Again with the condition $b > 1 + c$. We choose a first boundary segment B_0 as the $x = 0$ line, from $x = 0$ to some yet undefined value x_{bound}, since from our equations it is readily clear that the flow in this line goes upwards. The nullcline $y_1(x)$ becomes positive for values $x \geq \frac{1}{b+1}$ so we next define B_1 as a vertical segment going up from the point $(\frac{1}{b+1}, 0)$ until it meets the nullcline $y_2(x)$ at a value $y = \frac{b(b+1)}{c}$. On this segment, the $\dot{x}$ component of the flow field is always positive, since all points lie above the $\dot{x} = 0$ nullcline. The boundary segment B_2 is defined as a horizontal segment to the right of the point $(\frac{1}{b+1}, \frac{b(b+1)}{c})$. In this case, the flow is always downwards as all points are above the $\dot{y} = 0$ nullcline.

If we look at a line going downwards with a slope of -1, which has a normal vector (1, 1), the flow goes inwards if:

$$(1, 1) \cdot (\dot{x}, \dot{y}) = 1 - x \leq 0 \tag{5}$$

So, we extend the boundary B_2 until we reach a value $x = 1$, then we choose B_3 as a segment with normal (1, 1) from that point, until it hits the $\dot{x} = 0$ nullcline. We retrospectively define x_{bound} as the value at which this happens, and finally

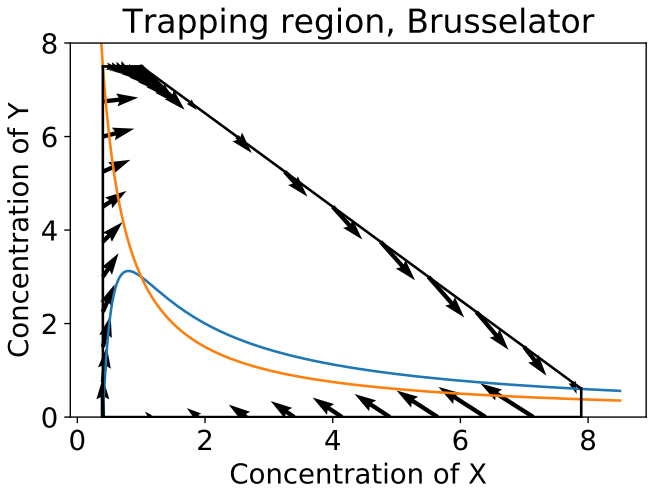

Figure 3: Representation of the trapping region for as described in the text. The nullclines are depicted as guidence. The vectors in the boundaries show that all the field point inwards, but the scale is altered for representation purposes.

define B_4 as a vertical segment from this point to the x-axis. Trivially, the flow points to the left at the latter. The trapping region is completed by removing the fixed point from the region, by defining a small circle around it. The resulting trapping region is depicted in Figure 3.

Establishing the existence of a periodic orbit in this fashion is only possible in principle for planar systems, where the Poincaré-Bendixon theorem is applicable. Moreover, constructing such a trapping region can be a formidable problem in general, so simple systems like the Brusselator present themselves as candidates upon which the analytical tools available can be developed to their fullest.

It is worth mentioning that the frequency of the oscillations can be approximated to zero-th order if the parameters are chosen above but very close to the Hopf bifurcation. Very close to the bifurcation value, the limit cycle is approximately a circle in phase space and it has a frequency coinciding with the imaginary part of the Jacobian eigenvalues in the equilibrium point. The validity of this result, though, is very limited, and in general the shape and period of the cycle must be determined from numerical integration methods.

Chemical reactions as stochastic processes

The more general and exact way to formalize a system of chemical reactions in a well-stirred mixture is as follows. Consider N molecular species $\{S_1, ..., S_N\}$ in a fixed volume Ω that react through M different reaction channels $\{R_1, ..., R_M\}$. The state of the system is represented by the state vector $\boldsymbol{X}(t) = (X_1(t), ..., X_N(t))$, i.e., the number of S_i molecules at time t -or similarly, the concentration vector

$\boldsymbol{x}(t) = \boldsymbol{X}(t)/\Omega$-.

We consider the reactions to happen at rates that only depend on the state vector (hence we do not consider temperature changes, e.g.). These rates can be well described by defining appropriate propensity functions $a_j(\boldsymbol{x})dt$ which give the probability that a reaction R_j will happen in the next time interval dt, given state $\boldsymbol{x}$. These propensity functions must be proportional to the number of ways in which the reactants of R_j may combine, $h_j(\boldsymbol{x})$. Thus, we can define $a_j(\boldsymbol{x}) = c_j h_j(\boldsymbol{x})$. The rate c_j has a dependency in the volume that depends on the number of reactants of R_j: the number of reactions per unit time should be proportional to Ω if molecule concentrations are kept constant. Thurefore, monomolecular reactions have a c_j that is independent of Ω, c_j is linear in Ω for bimolecular reactions, and so on.

The last quantity that determines our chemical reaction system is the stoichiometric matrix ν_{ji}, containing the change in number of S_i produced by one reaction R_j.

As defined, this system is a jump-type Markov process. Its conditioned probability function $P(\boldsymbol{x}, t|\boldsymbol{x}_0, t_0)$ is described by the chemical master equation [19]

$$\frac{\partial}{\partial t}P(\boldsymbol{x}, t|\boldsymbol{x}_0, t_0) = \sum_{j=1}^{M}\Big[a_j(\boldsymbol{x} - \boldsymbol{\nu}_j)P(\boldsymbol{x} - \boldsymbol{\nu}_j, t|\boldsymbol{x}_0, t_0) - a_j(\boldsymbol{x})P(\boldsymbol{x}, t|\boldsymbol{x}_0, t_0)\Big] \tag{6}$$

Master equations are, in general, difficult or impossible to solve or deal with. A reasonable approximation can be made if the system is reasonably represented by changing from a discrete space (molecule numbers) to a continuous one (concentrations).

Linear Noise Approximation (LNA)

For a volume Ω that is big enough (i.e. such that the changes due to single reactions represent very small changes to the molecule concentrations) we may approximate the chemical master equation 6 by a Fokker-Planck equation. The fundamental trick is to express the molecule numbers as

$$X_i(t) = \Omega\phi_i(t) + \frac{Z_i(t)}{\sqrt{\Omega}} = \Omega\phi_i(t) + \sqrt{\Omega}z_i(t)$$

Here, $\phi_i(t)$ represents the concentrations in the deterministic limit (obtained by the usual equations using mass-action kinetics) while $Z_i(t)$ is the contribution due to the noise, with the ansatz that the latter dies off as $\Omega^{-1/2}$. This ansatz is formally justified in [17] where the whole derivation is given.

The resulting Fokker-Plank equation (for the distribution of the displacement z_i away from the deterministic value) is

$$\frac{\partial Q}{\partial t} = -\sum_{i,j=1}^{N} J_{ij}(\boldsymbol{\phi})\frac{\partial}{\partial z_i}\big(z_j Q\big) + \frac{1}{2}\sum_{i,j=1}^{N} D_{ij}(\boldsymbol{\phi})\frac{\partial^2}{\partial z_i \partial z_j}Q \tag{7}$$

the first term on the r.h.s. is a drift term and the second one is a diffusive term. The matrices J_{ij} and D_{ij} are defined as:

$$\begin{aligned} J_{ij} &= \frac{\partial}{\partial \phi_j}\left(\frac{d\phi_i}{dt}\right) \\ D_{ij} &= \sum_{k=1}^{R} \nu_{ik} a_k(\boldsymbol{\phi}) \nu_{jk} \end{aligned} \tag{8}$$

The solution of a Fokker-Plank equation such as this one is a Gaussian, with zero mean (implying that the mean trajectory of an ensamble of realizations follows the deterministic mass-action equation) and a variance proportional to the matrix of covariances Ξ that is determined as [22]:

$$\frac{d}{dt}\Xi = J \cdot \Xi + \Xi \cdot J^T + D \tag{9}$$

The Gillespie algorithm

The Gillespie algorithm is an event-driven method used to computationally simulate Poisson processes [18]. Ideally, the method reproduces exactly the statistics of the time intervals between events, although numerical errors may arise due to the quality of the random number generators and round-off errors.

For any such process, M different events may be possible at any time (e.g. M different chemical reactions), each with an associated rate ν_i ($i = 0, ..., M-1$) that possibly depend on the state vector of the system at any given time. In this case, the rate at which an event happens is $\nu = \sum_i \nu_i$. With these definitions, the algorithm proceeds as follows:

1. Draw a random number τ from the distribution

$$P(\tau) = \nu e^{-\nu\tau}$$

2. Proceed by a time τ:

$$t \to t + \tau$$

3. Draw a random number a from a uniform distribution $U(0, \nu)$. Choose the event i such that

$$\sum_{j=0}^{i-1} \nu_j < a < \sum_{j=0}^{i} \nu_j$$

   And modify the state vector according to the chosen event.

4. Adjust the event rates to the new state vector and go back to (1).

As stated, the algorithm reproduces the process with exactitude. The comeback is that rates usually increase when the number of agents involved in the process grows, making the time between events increasingly small and thus simulations up to a final time T becoming increasingly slow. This usually limits simulations in chemical reactions systems (or similar) to some thousands of molecules.

Discrete stochastic processes such as Poisson processes define different regimes depending on the number of agents involved: very few agents make the process essentially discrete, while a mesoscopic number of them makes it possible to approximate the process to a continuous one up to a first order correction accounting for the stochastic nature of the process. Further on, we will see from the simulations performed for this work that the ranged of molecule numbers achieved with Gillespie's method is enough for the discussion that will follow, since the different regimes are all explored in such a range.

Limit-cycle oscillations: a phase description

The fact that periodic orbits are one-dimensional objects living in higher dimensional spaces appears as a key analytical tool for analysing their properties. Say we fix a starting point x_0 belonging to a limit cycle with period T as an initial condition for a trajectory, $x(t=0) = x_0$, hence we tag this point as $\theta = 0$. From here on, we let time go by and we tag all other points x in the cycle using the time taken by the trajectory to reach them, $\theta = t$, before getting back to x_0 at $t = T$. Each point in the cycle is now identified with a phase $\theta \in [0, T)$. A new phase $\phi(\theta)$ can always be defined such that it grows uniformly in time:

$$\frac{d\phi}{dt} = \omega_0 \tag{10}$$

where $\omega_0 = 2\pi/T$. This is achieved by the transformation:

$$\phi = \omega_0 \int_0^\theta \left[\frac{d\theta'}{dt}\right]^{-1} d\theta' \tag{11}$$

We now consider the effect of some external force or amount of noise as a small perturbation on the growth rate in this phase description:

$$\frac{d\phi}{dt} = \omega_0 + \epsilon g(\phi, t) \tag{12}$$

where the function $g(\phi, t)$ may depend on the phase itself, but also explicitly on time or on stochastic forces, and ϵ symbolically represents the smallness of the perturbation, though it will be set to unity in the end. A full description of $g(\phi, t)$ can be given in terms of local characteristics of the system when it is close to the limit-cycle in phase space, from the nature of the interactions and a description of the stochastic and external forces, as appropriate in every particular case.

Such an approach can be used to understand, for instance, how the stochastic forces affect the regularity of the period of an oscillator, as Kuramoto shows in

[7]. As a first approximation, imagine that the function $g(\phi, t)$ represents solely a random force which has zero mean and is Gaussian and delta-correlated, i.e.:

$$\langle g(\phi, t)\rangle = 0$$
$$\langle g(\phi, t)g(\phi, t')\rangle = 2D(\phi)\delta(t - t')$$

A system with such a stochastic differential equation is equivalent to the following Fokker-Planck equation, that describes the time evolution of the probability distribution for the state variables:

$$\frac{\partial P(\phi, t)}{\partial t} = -\frac{\partial I(\phi, t)}{\partial \phi} \tag{13}$$

with the probability flux $I(\phi, t)$ defined as

$$I(\phi, t) = \left(\omega_0 + \frac{\epsilon^2}{2}\frac{dD(\phi)}{d\phi}\right) P(\phi, t) - \epsilon^2 \frac{\partial}{\partial \phi}\left(D(\phi)P(\phi, t)\right)$$

Here the Stratonovich interpretation of the stochastic differential equation (SDE) is used, since we will be interested in modelling chemical reactions. The properties related to the phase shift are elucidated if the variable change $\phi = \omega_0 t + \psi$ is performed. Lets call $Q(\psi, t)$ the probability distribution for ψ which is obtained just by setting $P(\omega_0 t + \psi, t)$. Now the equation reads:

$$\frac{\partial Q(\psi, t)}{\partial t} = -\epsilon^2 \frac{\partial J(\psi, t)}{\partial \psi} \tag{14}$$

with the new probability flux

$$J(\psi, t) = \frac{1}{2}\frac{\partial D(\omega_0 t + \psi)}{\partial \psi} Q(\psi, t) - \frac{\partial}{\partial \psi}\left(D(\omega_0 t + \psi)Q(\psi, t)\right)$$

Now, it is clear that $Q(\psi, t)$ is a slowly varying function of time from its proportionality to ϵ^2, and we can therefore take the period-average of the quantities depending on $D(t + \psi, t)$ in the probability flux $J(\psi, t)$ as a good approximation, since those fluctuate much faster. The first of such terms vanishes as the average is taken, so we are left with the second term and the final averaged approximation reads (finally setting $\epsilon = 1$):

$$\frac{\partial Q(\psi, t)}{\partial t} = \bar{D}\frac{\partial^2}{\partial \psi^2}\left(Q(\psi, t)\right) \tag{15}$$

which is just a diffusion equation with constant:

$$\bar{D} = \frac{1}{T}\int_0^T D(\omega_0 t + \psi)dt$$

where T is the natural period of the oscillator. The diffusive behaviour is to be expected, since despite the presence of "forces" keeping the fluctuations from

growing in the transverse direction of the limit-cycle, there are no "forces" keeping those fluctuations tangent to the limit-cycle trajectory on check. In terms of stability quantities, this is equivalent to saying that one Lyapunov exponent (the one corresponding to the tangent direction in the periodic orbit) must be zero. Hence, fluctuations along that direction are totally equivalent to time shifts.

The implementation of such a phase-description needs a generalization of the concept of phase to points in the vicinity of the cycle, since an external forcing or random fluctuations may push the system away from the stable cycle. Such a generalization is provided by the concept of the *isochrones*. Take any point in phase space x such that a trajectory going through it approaches the cycle asymptotically as $t \to \infty$. We look at the stroboscopic mapping (with the oscillator's natural period T):

$$x(t) \to x(t + rT); \quad r \in \mathbb{N} \tag{16}$$

As a larger r is chosen, the endpoint lies closer to the cycle. We assign every point x with the phase ϕ corresponding to the point belonging to the cycle x_ϕ such that

$$x(t) \to x(t + rT) = x_\phi; \quad r \to \infty \tag{17}$$

Thus, if the cycle lives in a N-dimensional space, the subspaces with constant ϕ define $(N-1)$-dimensional surfaces, which are the aforementioned *isochrones*. A time shift Δt now transforms one isochrone ϕ to another one $\phi + \omega_0 \Delta t$; equivalently, small fluctuations locally transverse to the cycle conserve the isochrone, while those tangent to it represent a change of isochrone, equivalent to a time-shift.

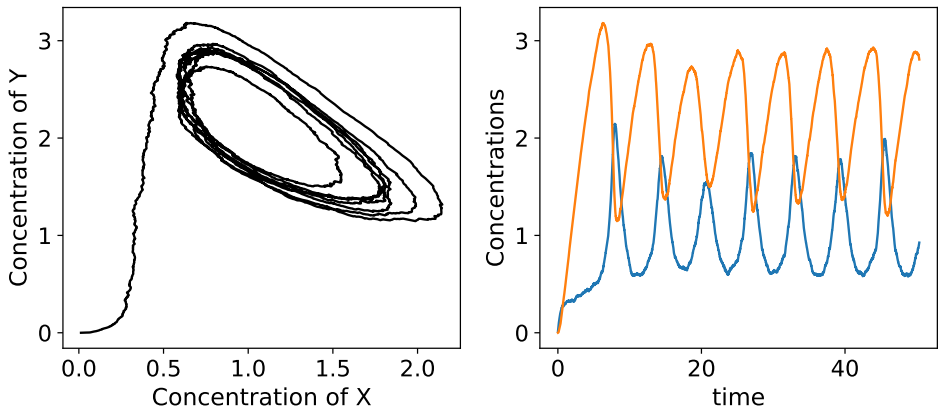

Figure 4: Sample trajectories for a Brusselator with intrinsic noise, for a volume V = 3000. Left: Phase-space trajectory. Right: Time evolution for both molecular species.

The phase-diffusion coefficient

The phase-diffusion coefficient D introduced in this section (omitting the average bar for the sake of further discussions) is probably the key concept upon which our work is built. We will see that this phase description of an oscillator is valid on the mesoscopic scale, failing at smaller scales where the demographic noise becomes too large and the clock does not stay close to the deterministic solution any more. In the case of a single oscillator and in such a mesoscopic scale, the value of D along with the natural period T of the cycle determine the period distribution completely. In this case, this distribution can be computed easily, as it will be shown at the beggining of part II in this work.

The consequences of phase-diffusion can be understood in the following way: take an ensemble of identical mesoscopic clocks. We let what would be a number r of deterministic periods take place, thus the time reaching the value rT ($r \in \mathbb{N}$). What is the ensemble average of the mean time given by the clocks? Since the process is diffusive it is the correct time,

$$\langle t_{clock} \rangle = rT \tag{18}$$

But how spread is the time in the ensemble? We can look at the variance around this mean value:

$$\langle (t_{clock} - rT)^2 \rangle^{1/2} = rD \tag{19}$$

It can be shown that this diffusion coefficient is inversely proportional to the extensivity parameter Ω in chemical systems (coloquially, the volume). The prefactor is then of most interest, since it is what depends on the dynamical properties of each specific clock.

The robustness of a cycle to stochastic fluctuations

Gaspard and others ([20], [21]) describes analytically how to compute the aforementioned prefactor if the limit-cycle trajectory is known. They term this quantity the 'robustness factor'. Indeed, it quantifies the statistical deviation of the period from its mean value due to a change in extensibility and its associated stochasticity. We will only sketch here some general ideas. The robustness of biochemical processes are of major importance also in other contexts, such as in regulatory biochemical networks [14].

Curiously enough, the WKB approximation used in quantum mechanics that maps quantum to classical optics can be used in the master equation of chemical systems in the mesoscopic scale to retrieve a Hamilton-Jacobi equation. A pseudo-energy functional E can be identified from here.

The resulting expression for the robustness factor depends essentially from how much a change in the pseudo-energy E makes the period vary, around the mean period T. This is:

$$\sigma^2 = \frac{\partial_E T}{\Omega} \tag{20}$$

With the important dependency $\sigma^2 \sim \Omega^{-1}$. The robustness factor $\partial_E T$ can be computed from quantities pertaining to the deterministic limit, such as the Jacobian and the noise-correlation matrices that may be integrated with a standard RK4, for instance. We do not use this approach on our work, though, σ^2 will be computed directly from numerical simulations of the stochastic system.

Noise-induced oscillations: Quasicycles

For a system to present a limit-cycle some dynamical features are needed. In planar systems specifically, the bounded region in phase space delimited by the cycle trajectory must include an unstable fixed point. However, if a controlling parameter is shifted below a critical value, this fixed point can be rendered stable (the limit-cycle becomes smaller until it merges with the fixed point). This is a Hopf bifurcation. However, for some region in parameter space, the eigenvalues of the Jacobian corresponding to this fixed point have an imaginary part, meaning that trajectories approaching it as time moves forward do so in a spiralling fashion, at least locally. When noise is included into the picture, one can imagine that random fluctuations keep the system from really reaching its otherwise stationary state, while still showing some cycling around it due to the local spiralling nature of the region in phase space.

The possibility of well defined, maintained oscillations in this sense has been formally and computationally explored by McKane et al. [12]. The authors use a linear noise approximation (LNA) to write a chemical Langevin equation, with also a linear approximation on some neighbourhood of the fixed point. They then use Fourier analysis to show that a peak in the Power Spectrum Density function of the system can exist, and therefore a resonant frequency is present in the system.

Using repeated indices as summations, the linearised Langevin equation can be written as follows:

$$\dot{x_i} = M_{ij} x_j + \eta_i(t) \tag{21}$$

where the variables x_i represent the concentrations and the origin is placed at the fixed point, the matrix M_ij is just de Jacobian evaluated at the origin and the terms $\eta_i(t)$ represent Gaussian forces with zero mean, delta-correlated in time and mutually correlated with matrix D_{ij}:

$$\langle \eta_i(t) \eta_j(t') \rangle = 2 D_{ij} \delta(t - t') \tag{22}$$

The diffusion matrix D_{ij} is determined from the stoichiometric coefficients and the reaction rates. Now, from this set of equations the Fourier transform is easily performed, readily giving:

$$-i\omega\hat{x}_i = M_{ij}\hat{x}_j + \hat{\eta}_i(\omega) \tag{23}$$

with correlations:

$$\langle\hat{\eta}_i(\omega)\hat{\eta}_j(\omega')\rangle = 2\pi D_{ij}\delta(\omega+\omega') \tag{24}$$

The left hand side can be expressed as $-i\omega\delta_{ij}\hat{x_j}$ using the Kronecker delta, therefore:

$$(-M_{ij} - i\omega\delta_{ij})\hat{x}_j = \hat{\eta}_i(\omega) \tag{25}$$

Now we may define the complex, frequency dependent matrix

$$\Phi(\omega) = -(M + i\omega I)^{-1} \tag{26}$$

which allows us to write:

$$\hat{x}_i = \Phi_{ij}(\omega)\hat{\eta}_j(\omega) \tag{27}$$

We are now ready to compute the power spectrum density by taking the ensemble average of the tensor product of the concentration vector (in the frequency domain):

$$\langle\hat{x}_i(\omega)\hat{x}_j^\dagger(\omega)\rangle = \Big(2\pi\delta(0)\Big)\Phi_{ik}(\omega)D_{kl}\Phi_{lj}^\dagger(\omega) \tag{28}$$

The proportionality factor $2\pi\delta(0)$ can be omitted on the account that this omission is accounted for when comparing to numerical estimations of the PSD. The proportionality factor is the time increment used in the sampling process in a discrete Fourier Transform computation.

In the obtained expression, the PSD of every subsequent chemical species are contained in the diagonal elements of the resulting matrix. It is worth noticing that the PSDs will be a division of polynomials in ω, with denominator being $|\det(M + i\omega I)|^2$ which is of degree $2n$ in ω (n being the number of chemical species), while the numerator will be of degree $2(n-1)$. Therefore, no matter the specificities of the model used, the PSDs will always decay asymptotically as $\sim \omega^{-2}$ when $\omega \to \infty$.

For some systems, within some range of parameter values, it can be shown that a maximum is present in the computed PSD for an amplified frequency ω^*.

Part III
Oscillations in two compartments

This section contains the main results of our work. The focus has been to explore different set-ups where two chemical oscillators got synchronized through a coupling mechanism, while maintaining the total volume of the system constant.

We first present the distribution of periods for the single oscillator, as a reference. Afterwards, we will present numerical results for the period distributions for the different coupled cases.

The distribution of periods for a mesoscopic clock

As it was promised in the above section, we can give an expression for the distribution of periods (or frequencies, for that matter) using the phase-description of an oscillator. As usual, this expression should be correct in the mesoscopic scale, where the phase picture of the oscillator is applicable also in the presence of population noise.

In this case, we face a first-passage time (FPT) problem: how much time does an oscillator, initially at $\phi = 0$, need to reach $\phi = 2\pi$? The distribution of such times is the first-passage-time distribution (FPTD) for $\phi = 2\pi$. The FPT problem is formulated by the PDE for $P(\phi, t)$ (equation 13) with an initial condition $P(\phi, t = 0) = \delta(\phi)$ and absorbing boundary condition $P(\phi = 2\pi, t) = 0$.

However, the absorbing boundary condition can be circumvented. The PDE can be solved without accounting for this condition if one adds a mirroring solution in the end that makes $P(\phi = 2\pi, t) = 0$ at all times. cite VanKampen

We can solve the problem for $Q(\psi, t)$ with no absorbing conditions and initial condition $Q(\psi, t = 0) = \delta(\psi)$. We get:

$$Q(\psi, t) = \frac{1}{\sqrt{2\pi D t}} \exp\left(- \frac{\psi^2}{4Dt} \right) \tag{29}$$

Changing $\psi = \phi - t$ we get the distribution for $P(\phi, t)$ with initial condition $P(\phi, t = 0) = \delta(\phi)$. We are also interested in adding a solution that cancels the probability at $P(\phi = T, t)$ to get the solution for the absorbing boundary problem. The result is:

$$P_{abs}(\phi, t) = \frac{1}{\sqrt{4\pi D t}} \left[\exp\left(- \frac{(\phi - t)^2}{4Dt} \right) - \exp\left(- \frac{(\phi + t - 2T)^2}{4Dt} \right) \right] \tag{30}$$

It is easy to proof by inspection that this solution satisfies the corresponding PDE, that $P(\phi = T, t) = 0$ and $P(\phi, t = 0) = \delta(\phi)$. Now, the FPTD is equal to the flux of probability at $\phi = T$, so:

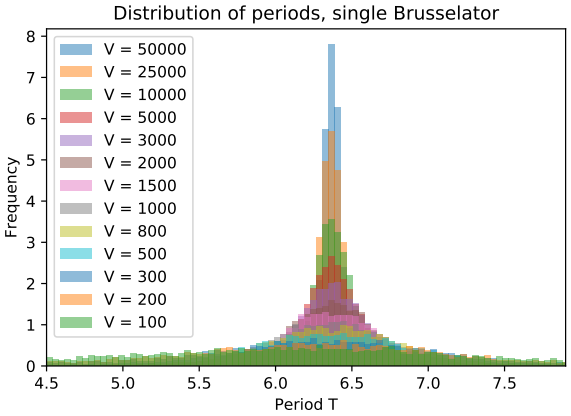

Figure 5: Numerically computed distribution of periods (normalized) for a single Brusselator above the Hopf bifurcation, with parameters $b = 2.2$ and $c = 1$. We observe a dependency of the broadness of the distribution with volume.

$$P_{fpt}(t) = \frac{T}{\sqrt{4\pi D t^3}} \exp\left(- \frac{(t-T)^2}{4Dt} \right) \tag{31}$$

[ref VanKampen]

This is the same distribution as for a brownian particle to reach the bottom of a container under the effect of gravity. In figure 5 we show the numerically computed distribution for a series of volumes.

Additionally, we should expect the phase diffusion coefficient D to have a dependency $D \sim V^{-1}$ in the mesoscale, as found by Gaspard et al and explained in equation 20. This allows us to roughly compute the robustness factor by fitting the obtained distribution (Eq. 31) distribution. We illustrate this in figure 6 by fitting the distribution to the obtained data for $V = 25000$ and then rescaling D to fit $V = 50000$.

We can relate the phase-diffusion D with the moments of the distribution. In terms of the standard deviation σ and mean μ:

$$\begin{aligned} \mu &= T \\ \sigma^2 &= 2DT \end{aligned} \tag{32}$$

We should expect any clock in the mesoscopic scale to be approximated by these expressions, even when we consider coupled cases. A basic assumption is then that the coupling considered in our clocks do not modify the deterministic trajectories by much, hence leaving the mean period almost unchanged, and we focus on the effect of the coupling in the phase-diffusion coefficient.

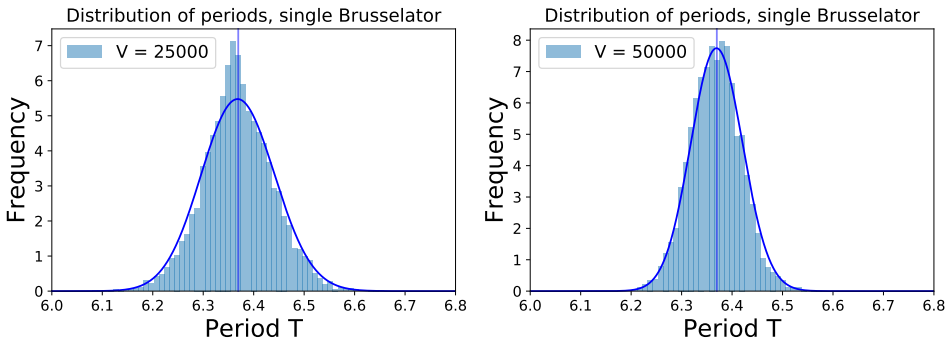

(a) (b)

Figure 6: (a) Detail of the distribution depicted in figure 5 for volume = $2.5 \cdot 10^4$. The solid line is a plot of the first-passage time density as expressed in equation 31, using the mean of the numerical distribution as T ($T_{mean} = 6.36$, vertical line) and fitting a value for $D = 10.4/(2.5 \cdot 10^4)$. (b) Detail of the distribution for volume = $5 \cdot 10^4$. Here the solid line takes the parameters already obtained in figure (a), with a proper rescaling of the diffusion coefficient $D = 10.4/(5 \cdot 10^4)$, which illustrates the dependency $D \sim V^{-1}$.

Concentration-driven transport, symmetric case

The first configuration we tried is quite simple: let us divide the volume in two equal compartments, then introduce some transport between compartments that is proportional to the concentration of each chemical species. This is what we should expect for a membrane with passive transport, with molecules crossing the membrane with a certain rate if they bump onto it.

The equations representing this system are the following:

$$\begin{aligned}
\dot{x} &= 1 + cx^2y - (b+1)x - k_1(x-u) \\
\dot{y} &= -cx^2y + bx - k_2(y-v) \\
\dot{u} &= 1 + cu^2v - (b+1)u + k_1(x-u) \\
\dot{x} &= cu^2v - bu + k_2(y-v)
\end{aligned} \tag{33}$$

We term this configuration 'symmetric' since exchanging the names of the compartments leaves the system unchanged.

Dynamical analysis

The dynamical analysis in this case gets much more complicated than for the single oscillator, since the system is no longer planar and the Poincaré-Bendixon theorem does not apply. The dynamics of 4D systems are much richer in behaviour. Nev-

ertheless, we can point out some facts using LSA and rely on some numerical integration to explore the system a bit further.

It is clear that the fixed point for the single system $(1, b/c)$ is still a fixed point, since the coupling terms cancel there. We can look for the stability of this fixed point, again computing the Jacobian. This can be done in a rather compact way if we define the matrix $\kappa = diag(k_1, k_2)$ and use the original Jacobian μ^* (Equation 2). Then, in block-matrix notation, the Jacobian is:

$$M = \begin{pmatrix} \mu - \kappa & \kappa \\ \kappa & \mu - \kappa \end{pmatrix} \tag{34}$$

This notation allows to easily perform some row and column operations that factorizes the characteristic equation $\det(M - \lambda I_4) = 0$:

$$\begin{vmatrix} \mu - \kappa - \lambda I_2 & \kappa \\ \kappa & \mu - \kappa - \lambda I_2 \end{vmatrix} = \begin{vmatrix} \mu - \lambda I_2 & \kappa \\ \mu - \lambda I_2 & \mu - \kappa - \lambda I_2 \end{vmatrix} = \\ \begin{vmatrix} \mu - \lambda I_2 & \kappa \\ 0 & \mu - 2\kappa - \lambda I_2 \end{vmatrix} = \det(\mu - \lambda I_2) \det(\mu - 2\kappa - \lambda I_2) = 0 \tag{35}$$

The first factor indicates that the original eigenvalues are conserved after the coupling. The second factor introduces two new eigenvalues. We now use Δ and τ as before for the determinant and trace of μ, and $\hat{\Delta}$, $\hat{\tau}$ respectively for $\mu - 2\kappa$. They are related as:

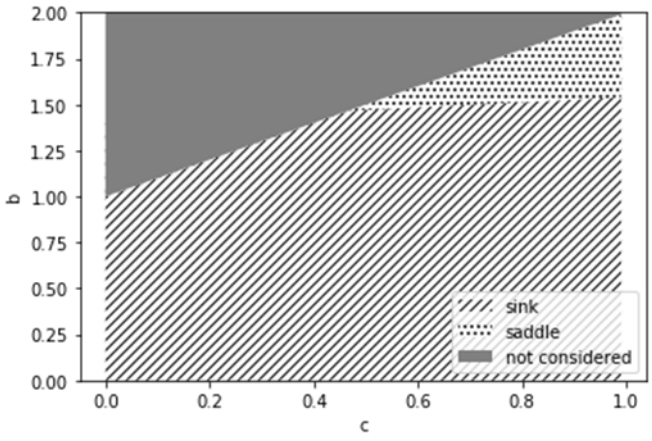

Figure 7: White background region – the Brusselators were stable before coupling. In the dotted region the fixed point becomes a saddle (the boundary with the stripped region is a pitch-fork bifurcation). Grey region – the Brusselators were unstable before coupling. This case is still considered in the LSA.

$$\begin{aligned} \hat{\Delta} &= \Delta - 2(b-1) + 2c + 4k_1k_2 \\ \hat{\tau} &= \tau - 2(k_1 + k_2) \end{aligned} \tag{36}$$

Clearly, the trace $\hat{\tau}$ is always negative provided that the original trace τ is also negative. Hence, if the Brusselators are originally in the stable regime, the fixed point will be stable after the coupling if $\hat{\Delta} > 0$, that after some rearranging gives the relation:

$$b < \frac{1 + 2k_1}{2k_2} c + 1 + 2k_2 \tag{37}$$

In parameter space (b, c) (assuming some fixed k_1, k_2), this condition is a straight line: if b is below this line, while fulfilling $\tau = b - 1 - c < 0$ at the same time (which is also a straight line), the fixed point remains locally stable. This is illustrated in figure 7.

Another way of phrasing this condition is that the system will have some positive eigenvalue (given that $\tau < 0$) only if

$$k_2 - k_1 > \frac{1}{2} \tag{38}$$

This relation will proof of some importance when exploring the coupled system in the quasicycle regime, since it is indicative that the quasicycles happen about the same fixed point as the original system. The fact that at least $k_2 > 1/2$ is necessary for the change in stability proves good: stability will not change with finite values of the coupling constants k_1, k_2, at least in some range.

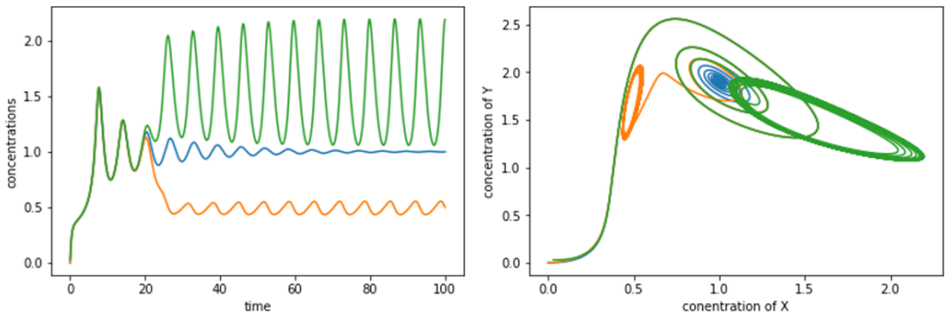

(a) (b)

Figure 8: (a) Concentration of X in a single stable Brusselator (blue) and two coupled Brusselators in the dotted region (green and orange, for each compartment). Parameters are $b = 1.9$, $c = 1$ and coupling constants $k_1 = 0$ and $k_2 = 3$. We observe that, while the oscillations in the single Brusselator die off, they persist after the coupling. (b) Projection in the X-Y plane of the single Brusselator trajectory and coupled Brusselator

In the doted region in figure 7, the fixed point becomes a saddle. Numerical integration indicates that at least two new fixed points exist, and suggest that they are either stable or unstable, in which case the system undergoes a Hopf bifurcation. This could result in the curious case in which two stable Brusselators couple to result in a limit cycle oscillator. We illustrate this in figures 8a and 8b.

Numerical results

This system was simulated for different volumes, using a Gillespie algorithm. We will refer to the 'volume' as to the sum of volumes of all compartments. This way, the average number of molecules is conserved as a whole when the compartmentalization is performed. However, we should expect each compartment to be more noisy on its own, since the extensivity is reduced.

We compute the standard deviation σ of the period distribution from the numerical results obtained. The coefficient of phase-diffusion D is thereby obtained making use of equation 32. We plot the computationally obtained Ds as a function of the volume in figure 9, in logarithmic scale, and use a regression of the type $D = a/V$ (solid line) only with the bigger volumes. We observe that the periods seem to distribute to the computed PDF (eq. 31) only for volumes $> 10^3$ approximately.

It is clear from the plot, and from the obtained robustness factors, that the oscillations are more robust in the face of noise for the single than for the coupled case. This results may not make a general case at all, since many parameters have been chosen arbitrarily. In the coming section, we give an argument on why we have not observed this sort of coupling succeed even when trying for different parameter values. This argument must be considered heuristic, since the phase-description used in it is not an exact match of our chemical system.

An heuristic argument using Langevin equations

Let us first look, in the phase description scheme, at the coupling of two oscillators with the only constraint that the coupling functions depend on the phase difference for each pair of oscillators, and it does so with an odd symmetry, $\Gamma(\phi_1 - \phi_2) = -\Gamma(\phi_2 - \phi_1)$. In other words, the coupling strengths break the compartment symmetry. We will afterwards get rid of this asymmetry to look at the case of n oscillators.

Now, we can write coupled Langevin equations for the phases:

$$\begin{aligned} \dot{\phi}_1 &= \omega_1 + K_1\Gamma(\phi_2 - \phi_1) + \xi_1(t) \\ \dot{\phi}_2 &= \omega_2 + K_2\Gamma(\phi_1 - \phi_2) + \xi_2(t) \end{aligned} \tag{39}$$

Where the $\xi_i(t)$ represent some white noise functions.

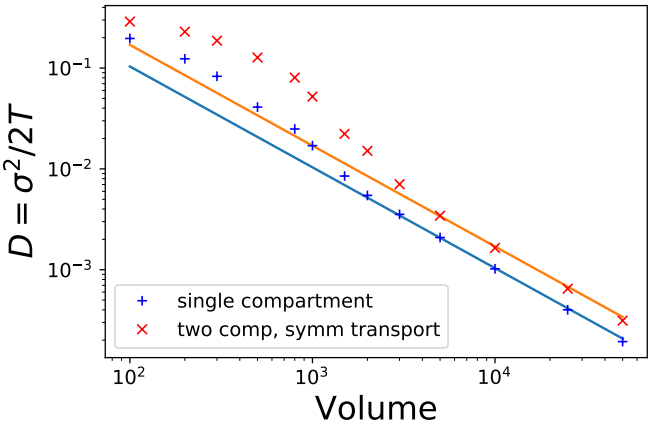

Figure 9: Numerically computed phase-diffusion coefficients as a function of the volume. The chemical system is simulated using a Gillespie algorithm and then the periods are computed from the obtained timeseries. Blue: single brusselator. Red: symmetrically coupled brusselators, as described in this section. The solid lines are fits to the function $D = a/V$, and only the bigger volumes are used (mesoscale and above). The regressions give, $a = 10.38$ and $a = 16.99$ for the single and coupled cases, respectively.

This description is not an exact match of our chemical system, since here the coupling functions depend only in the difference in phase, and the coupling in the original chemical system depends on the distance in phase space. We should expect the description given here to be a better one for increasing volumes, since the fluctuations away from the limit-cycle become increasingly smaller and thus the coupling is mostly dependent on where in the cycle the system is, and not so much on how far from it.

With a smart combination of the equations, one can get one equation without any nonlinear terms, which will therefore be a simple diffusive variable. This is achieved if one computes the centre-of-mass analogue for the phases:

$$\theta = \frac{K_2\phi_1 + K_1\phi_2}{K_1 + K_2} \tag{40}$$

The equation for θ is:

$$\dot{\theta} = \omega + \xi(t); \quad \omega = \frac{K_2\omega_1 + K_1\omega_2}{K_2 + K_1} \tag{41}$$

And the diffusion constant for this variable becomes:

$$\hat{D} = \frac{1}{2}\langle \xi(t)^2 \rangle = \frac{K_2^2 D_1 + K_1^2 D_2}{(K_1 + K_2)^2} \tag{42}$$

We could look at this last equation from another perspective if we set a mean $K = (K_1 + K_2)/2$ to fix a scale of the coupling strength and then use $\Delta K = (K_2 - K_1)/2$ as a measure of the possible asymmetry in the coupling. It must be emphasized that the picture we are painting does not completely match our system as described in this section. Now, we imposed from the very beginning that the compartments should not be distinguishable. In that case, we should impose $K_1 = K_2$ to get a more reasonable picture. Not imposing this condition, the dynamical properties of the system (i.e. the dynamical characteristics of the deterministic equations) may be completely different.

That very small values of ΔK should not change dramatically the dynamical properties of the system is not an unreasonable assumption to make. Imposing that the two systems have equal diffusion constants, and that these are doubled with respect to their original ones after the coupling, $D_1 = D_2 = 2D$ -since the effective volume is halved-, we arrive at:

$$\hat{D} = 2D\frac{(K + \Delta K)^2 + (K - \Delta K)^2}{4K^2} = D\left(1 + \frac{\Delta K^2}{K^2}\right) \tag{43}$$

So, now adjusting to the case where $\Delta K = 0$, we see that the diffusion coefficient remains unchanged. This is, however, the diffusion coefficient for the 'centre of mass' of the oscillators, and we must remember each oscillator also fluctuates around the centre of mass, so we should expect the actual diffusion coefficient to be bigger in the coupled case. This is what we see from our computational results presented previously.

As discussed, though, we should expect equation 43 to hold at least for small asymmetries in the coupling strength. If this is actually the case, $\Delta K = 0$ is the minimum of a parabola, so we should expect the coupled diffusion constant to be even bigger if these asymmetries are introduce. In other words, the symmetric coupling seems to maximize -at least locally- the quality of the oscillations. But it does not do the trick.

Coupled chemical oscillators: asymmetric case

We investigated a setup where one compartment (A) is capable of sending molecules of the type X to the other comparment (B), while compartment A remains unaware of what happens in B. If the subscripts 1 and 2 refer to molecules in compartment A or B respectively, the differential equations representing this system would be:

$$\begin{aligned}
\dot{x}_1 &= a - bx_1 + x_1^2 y_1 - x_1 - Kx_1 \\
\dot{y}_1 &= bx_1 - x_1^2 y_1 \\
\dot{x}_2 &= a - bx_2 + x_2^2 y_2 - x_2 + Kx_1 \\
\dot{y}_2 &= bx_2 - x_2^2 y_2
\end{aligned} \tag{44}$$

Numerical Results

We simulated this system using the Gillespie algorithm with parameters $a = 2, b = 6, K = 0.2$ and for a wide range of volumes. As shown in the figure, one observes an apparent improvement regarding the standard deviation of the periods in compartment A. However, compartment A is independent of whatever happens at B, so

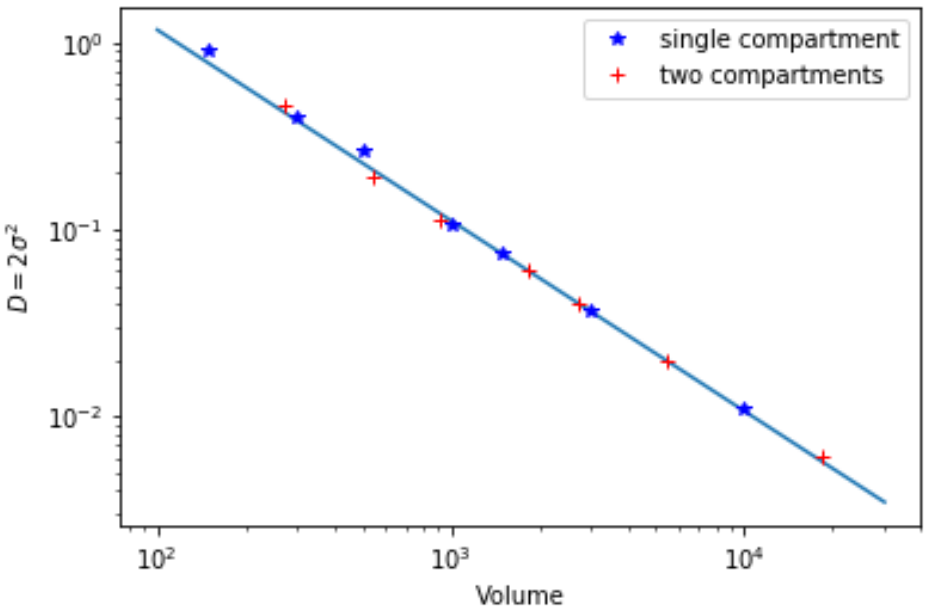

Figure 10: Blue dots: two comparments, standard deviation of the period distribution for the X molecules in compartment A, with $a = 2, b = 6$. Red dots: single comparment with modified parameters $\hat{a}, \hat{b}$, standard deviation of the X molecules, after rescaling volume and time.

we must attribute this improvement only to the effect of the term $-Kx_1$ in the first equation.

Coupling as a parameter shift

The addtion actually represents a change in the dynamical parameters a, b since the extra term disappears after a proper change in dimensions of time and space. If we focus only in the first equation and define new dimensions of time such that $t \to (1+K)t$ and $V \to V/\sqrt{1+K}$ (this last change reflecting on the concentrations), it becomes:

$$\dot{x}_1 = \hat{a} - \hat{b}x_1 + x_1^2 y_1 - x_1$$

where

$$\hat{a} = \frac{a}{(1+K)^{3/2}}, \qquad \hat{b} = \frac{b}{1+K}$$

Therefore, the first two equations are equivalent to our usual Brusselator system, now with parameters $\hat{a}, \hat{b}$ and with rescaled dimensions. Note that a similar argument could be applied if the transported molecules had been of the Y type instead of X. To check the validity of this argument we performed a simulation with a single compartment, now with the modified parameters, and compared to our previous results with two compartments. We can see (figure) that, after scaling the dimensions properly, the standard deviations seem very much to fall onto the same curve as before. This indicates that the improvement was not due to the comparmentalization but to a more suitable dynamical parameters.

Yet, a plausible mechanism for improvement of the period regularity would be to use one compartment as a 'dump-site' where to send some excess of molecules and improve the system as it has been described. Biologically, though, this could seem more complicated and not as efficient as fine-tunning the parameters and using the whole volume for the oscillator, an alternative that appears evolutionarily more plausible. x

Part IV
Quasicycles in two compartments

Limit-cycles are not the only way to generate coherent and sustained oscillations, as we already mentioned. If a system is to approach a stable fixed point in the deterministic limit, the addition of intrinsic noise keeps pushing the system out of this fixed point. A proper dynamical neighbourhood of the fixed point may induce this travels in the phase space to do so in a more or less coherent way around it, giving rise to oscillations.

The contribution of noise to the oscillations in this case is crucially different from that on the limit-cycle case. Now, without noise there are no oscillations, since the system approaches the fixed point and stays there. In the limit-cycle case, noise can be regarded as a disruptive effect on the quality of biological clocks. In this case, noise is an indispensable ingredient to obtain oscillations.

The distribution of periods for quasicycles

One principal difference that we notice between limit-cycle oscillations and quasicycles is the distribution of periods. We have seen, analytically and computationally, that the periods for limit-cycle-like clocks distribute more sharply around the mean value for increasing volumes (ref to figures and eq). This appears not to be the case for quasicycles: the distribution of periods does not depend in the volume. We show this computationally, by running a series of Gillespie simulations on a Brusselator system with parameters below the Hopf bifurcation, for several volumes. The results are shown in Figure 12 where we see that the different distri-

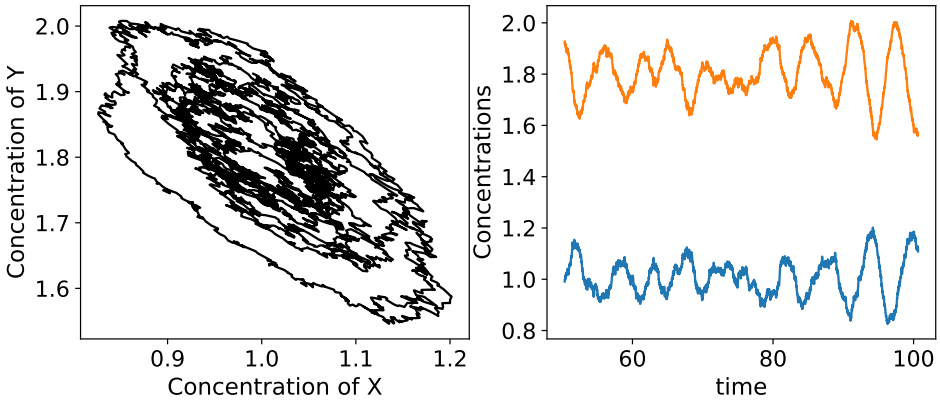

Figure 11: Trajectories for a Brusselator in the quasicycle regime. Left: phase-space. Right: Time evolution for both chemical species. Some coherence in revolving around the fixed point is already apparent.

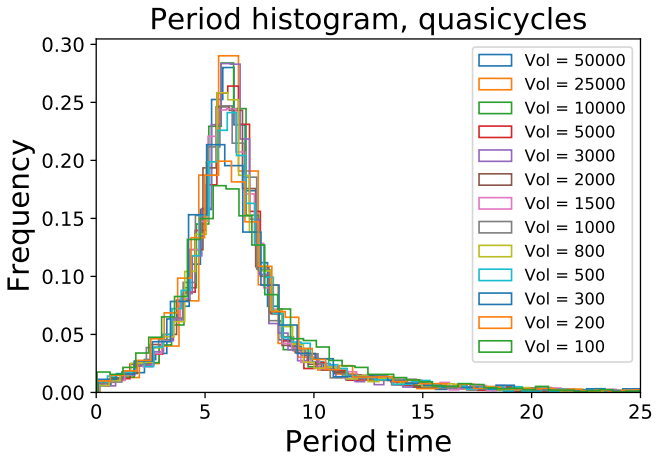

Figure 12: Obtained distribution of periods for Gillespie simulations of the Brusselator in a quasicycle regime. There are no appreciable differences for the different volumes that were simulated.

butions overlap.

In this case, one has to look at the distribution of amplitudes for the oscillations in order to see how these are shut down as the deterministic limit is approached (Figure 13). In the mesoscopic scale, we should expect (as was explained in the preliminaries section) the distribution in the stationary state to be a multivariate Gaussian centred in the fixed point with some standard deviation that is smaller for bigger volumes.

Power Spectrum Density for coupled quasicycles

Following the derivation of McKane [12] of the power spectrum density for quasi-oscillatory chemical systems, the aim of this derivation is to compute a modified power spectrum density for two chemical systems that are diffusively coupled by means of a membrane between two compartments. The coupling depends on a transport rates K_i; the power spectrum density in the limit $K_i \to 0$ must recover the result given at McKane.

As an example, take the Brusselator system in the stable regime, represented by the following set of differential equations in the deterministic limit:

$$\begin{aligned} \dot{x} &= a + x^2 y - bx - x \\ \dot{y} &= -x^2 y + bx \end{aligned} \tag{45}$$

Now, the interest is to couple two such systems, in equal compartments A and B,

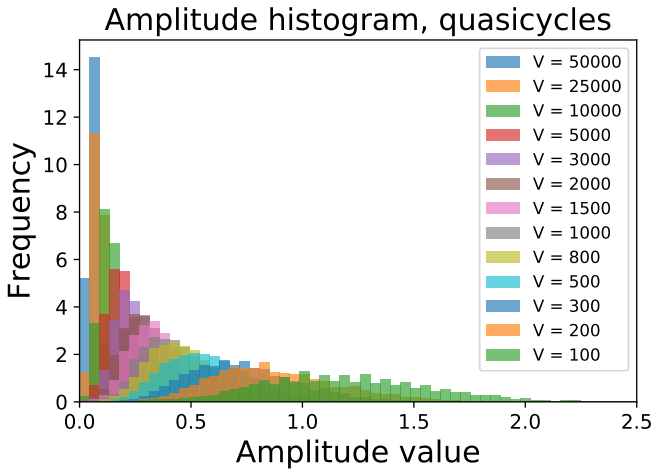

Figure 13: Histograms for the amplitude distributions obtained using Gillepsie simulations for the same Brusselator as in Figure 12. Clearly, the distribution jams up around 0 for big volumes.

each with half the volume of the entire system.Then we get the related system:

$$\begin{aligned}
\dot{x_1} &= a + x_1^2 y_1 - b x_1 - x_1 + K_x(x_2 - x_1) \\
\dot{y_1} &= -x_1^2 y_1 + b x_1 + K_y(y_2 - y_1) \\
\dot{x_2} &= a + x_2^2 y_2 - b x_2 - x_2 - K_x(x_2 - x_1) \\
\dot{y_2} &= -x_2^2 y_2 + b x_2 - K_y(y_2 - y_1)
\end{aligned} \tag{46}$$

The single system has a fixed point $(x^*, y^*) = (\alpha, \beta/\alpha)$ that is stable for $\beta < 1 + \alpha^2$. Note that the same point is also a fixed point for the coupled systems, since the coupling terms vanish if the analogous variables are equal. (Stability conditions can change right? I must check this.)

The stability matrix of the system is defined as:

$$\boldsymbol{M}_{ij} = \frac{\partial f_i(x)}{\partial x_j} \tag{47}$$

and it is also useful to define the stoichiometric matrix $\boldsymbol{S}_{ij}$, which gives the change in one species i by a reaction channel j; and the rate vector ν_j that gives the rate constant of reaction channel j. Then, the result given by McKane for the psd is given by:

$$P_i(w) = \left(\boldsymbol{\Phi}(w)^{-1} \cdot \boldsymbol{B} \cdot \boldsymbol{\Phi}^{\dagger}(w)^{-1}\right)_{ii} \tag{48}$$

meaning the psd of component i is given by the element ii of the matrix in brackets, and $\boldsymbol{\Phi} = -iw\boldsymbol{I} - \boldsymbol{M}$ ($\boldsymbol{I}$ the identity matrix), $\boldsymbol{B} = \boldsymbol{S} \cdot diag(\boldsymbol{\nu}) \cdot \boldsymbol{S}^T$ is the noise-correlation matrix, $diag(\boldsymbol{\nu})$ is the matrix that has the reaction rates on the diagonal, and $\boldsymbol{\Phi}^{\dagger}(w) = \boldsymbol{\Phi}^T(-w)$ denotes de adjoint matrix.

Since the system-size expansion is used to derive this equations, they are valid only for big-enough volumes.

Frequency and peak shift

We can express the PSD of the coupled systems in the symbolic form:

$$\hat{P}(w) = P(w) + \epsilon f(w) + O(\epsilon^2) \tag{49}$$

where the hat indicates the perturbed system (the two coupled compartments).

Say that $P(w)$ had an amplified frequency $w = w^*$, meaning that $P(w^*)$ is a maximum. How does the maximum shift with the perturbation? How is the height of the maximum affected by the shift?

Define the shifted frequency as $\hat{w}^* = w + \epsilon$. Now, take derivatives on both sides and demand that they vanish at $w = \hat{w}^*$. Assuming ϵ is small, the first terms in a Taylor expansion around $w = w^*$ are the relevant ones.

$$\frac{d\hat{P}(w)}{dw}\Big|_{w=w^*+\epsilon} \approx \epsilon \frac{d^2P(w)}{dw^2}\Big|_{w=w^*} + K\frac{df(w)}{dw}\Big|_{w=w^*} + K\epsilon\frac{d^2f(w)}{dw^2}\Big|_{w=w^*} = 0 \tag{50}$$

The solution for ϵ, to first non-vanishing order in D, is:

$$\epsilon = -K\frac{f'(w^*)}{P''(w^*)} + O(K^2) \tag{51}$$

Which is consistent with the assumption that ϵ is small, since ϵ is order K. Now, the value of the peak at the maximum is also modified:

$$\hat{P}(w^* + \epsilon) = P(w^*) + Kf(w^*) + O(K^2) \tag{52}$$

So, basically, the peak should be higher (hence more amplified frequency? is this condition enough?) it the value of $f(w)$ is positive at the unperturbed resonant frequency.

It is also possible to compute the factor of resonance R as defined in McKane [12]:

$$\hat{R} = \frac{\hat{P}(\hat{w}^*)}{\hat{P}(0)} \approx \frac{P(w^*) + Kf(w^*)}{P(0) + Kf(0)} \approx \frac{P(w^*) + Kf(w^*)}{P(0)}(1 - Kf(0)) \tag{53}$$

with the result

$$\hat{R} = R(1 - Kf(0)) + K(\frac{f(w^*)}{P(0)}) \tag{54}$$

Calculations

Now, note that it is possible to write all the necessary matrices for the coupled case in terms of the matrices of the single compartment case. From here on, lower case Greek letters $\boldsymbol{\mu}$, $\boldsymbol{\beta}$ and $\boldsymbol{\phi}$ will correspond to the single-compartment case -$\boldsymbol{\mu}$ the stability matrix, $\boldsymbol{\beta}$ the noise-correlation matrix, and $\boldsymbol{\phi}(w) = -iw\boldsymbol{I} - \boldsymbol{\mu}$-, while $\hat{\boldsymbol{M}}$, $\hat{\boldsymbol{B}}$ and $\hat{\Phi}$ refer to the coupled-systems' matrices respectively. Then we can write, in block matrices notation:

$$\hat{\boldsymbol{M}} = \begin{pmatrix} \boldsymbol{\mu} - \boldsymbol{\kappa} & \boldsymbol{\kappa} \\ \boldsymbol{\kappa} & \boldsymbol{\mu} - \boldsymbol{\kappa} \end{pmatrix} \tag{55}$$

$$\hat{\boldsymbol{B}} = \begin{pmatrix} \boldsymbol{\beta} + 2\boldsymbol{\kappa} & -2\boldsymbol{\kappa} \\ -2\boldsymbol{\kappa} & \boldsymbol{\beta} + 2\boldsymbol{\kappa} \end{pmatrix} \tag{56}$$

$$\hat{\Phi}(w) = \begin{pmatrix} \boldsymbol{\phi}(w) + \boldsymbol{\kappa} & -\boldsymbol{\kappa} \\ -\boldsymbol{\kappa} & \boldsymbol{\phi}(w) + \boldsymbol{\kappa} \end{pmatrix} \tag{57}$$

where $\boldsymbol{\kappa} = diag(K_i)$. The derivation of the matrix $\boldsymbol{B}$ is in another section. It is useful at this point to define the coupling matrix

$$\mathcal{K} = \begin{pmatrix} \boldsymbol{\kappa} & -\boldsymbol{\kappa} \\ -\boldsymbol{\kappa} & \boldsymbol{\kappa} \end{pmatrix} \tag{58}$$

so as to express $\hat{\Phi}(w) = \Phi(w) + \boldsymbol{\mathcal{D}}$ and $\hat{\boldsymbol{B}} = \boldsymbol{B} + 2\boldsymbol{\mathcal{D}}$, where the matrices without the hat recover those of two uncoupled systems. Now we want to compute the matrix $\hat{\mathcal{P}}(w) = \hat{\boldsymbol{\Phi}}(w)^{-1}\hat{\mathbf{B}}\hat{\boldsymbol{\Phi}}^{\dagger}(w)^{-1}$. It is possible to express the two inverse matrices involved in this product in terms of the uncoupled matrices using the following general result for any two invertible matrices A and B:

$$\begin{aligned} &(A+B)^{-1}(A+B) = I \\ &\Rightarrow (A+B)^{-1}A = I - (A+B)^{-1}B = I - A^{-1}(I+BA^{-1})^{-1}B \\ &\Rightarrow (A+B)^{-1} = A^{-1} - A^{-1}(I+BA^{-1})^{-1}BA^{-1} \end{aligned} \tag{59}$$

A small parameter ϵ can be introduced as follows:

$$(A+\epsilon B)^{-1} = A^{-1} - \epsilon A^{-1}(I+\epsilon BA^{-1})^{-1}BA^{-1} \tag{60}$$

and the formula can be recursively used for the term in the rhs $(I+\epsilon BA^{-1})^{-1}$:

$$(I+\epsilon BA^{-1})^{-1} = I - \epsilon(I+\epsilon BA^{-1})^{-1}BA^{-1} = I + O(\epsilon) \tag{61}$$

So, up to first order in the perturbation parameter:

$$(A+\epsilon B)^{-1} = A^{-1} - \epsilon A^{-1}BA^{-1} + O(\epsilon^2) \tag{62}$$

This result applied to the case at hand yields:

$$
\begin{aligned}
&\hat{\mathcal{P}}(w) = \\
&= \left(\Phi(w)^{-1} - \Phi(w)^{-1}\mathcal{K}\Phi(w)^{-1}\right)(\boldsymbol{B} + 2\mathcal{K})\left(\Phi^{\dagger}(w)^{-1} - \Phi^{\dagger}(w)^{-1}\mathcal{K}\Phi^{\dagger}(w)^{-1}\right) \\
&= \mathcal{P}(w) + 2\Phi(w)^{-1}\mathcal{K}\Phi^{\dagger}(w)^{-1} - \Phi(w)^{-1}\mathcal{K}\mathcal{P}(w) - \mathcal{P}(w)\mathcal{K}\Phi^{\dagger}(w)^{-1} + O(K^2)
\end{aligned}
\tag{63}
$$

To this point, all the derivations should be valid in general: for any pair of equal systems of chemical reactions coupled with a diffusive membrane. All the relevant information concerning the PSDs is contained in the top-left block, since equal chemical species in different compartments should have the same PSD and those are contained in the diagonal. In the case of our two coupled Brusselators, we can solely compute the 11 component of the matrix $\hat{\mathcal{P}}(w)$ to obtain $\hat{P}_x(w)$, and the result for $\hat{P}_y(w)$ is retrieved by changing subindices $x \leftrightarrow y$ and $1 \leftrightarrow 2$.

$$
\Delta P_x(w) = \frac{1}{|det(\boldsymbol{\phi})|^2}\left(K_x|\phi_{22}|^2 + K_y|\phi_{12}|^2\right) - 2\left[K_x P_x \operatorname{Re}\left(\frac{\phi_{22}}{\det\phi}\right) + K_y \operatorname{Re}\left(\frac{P_{xy}^{*}\phi_{12}}{\det\phi}\right)\right]
\tag{64}
$$

We can have a look on how this would look like, e.g., for $K_y = 0$. The different terms then are:

$$
2K_x\frac{|\phi_{22}|^2}{|\det\Phi|^2} = 2K_x\frac{M_{22}^2 + w^2}{(\Delta - w^2)^2 + \tau^2 w^2}
$$

$$
-2K_x P_x \operatorname{Re}\frac{\phi_{22}}{\det\Phi} = 2K_x\frac{B_{11}w^2 + \alpha}{(\Delta - w^2)^2 + \tau^2 w^2}\frac{M_{22}(\Delta - w^2) + \tau w^2}{(\Delta - w^2)^2 + \tau^2 w^2}
$$

$$
\alpha = B_{11}M_{22}^2 + B_{22}M_{12}^2 - 2B_{12}M_{12}M_{2}2
$$

And then plot the computed PSD as in figure 14.

Derivation of the noise-correlation matrix $\boldsymbol{B}$

Again, the use of block matrices comes handy. The stoichiometric matrix $\boldsymbol{S}$ of the coupled systems may be expressed in terms of the single-system one $\boldsymbol{\sigma}$ as:

$$
\boldsymbol{S} = \begin{pmatrix} \boldsymbol{\sigma} & 0 & \boldsymbol{I}_2 & -\boldsymbol{I}_2 \\ 0 & \boldsymbol{\sigma} & -\boldsymbol{I}_2 & \boldsymbol{I}_2 \end{pmatrix}
\tag{65}
$$

note that $\boldsymbol{\sigma}$ is a 4×2 matrix while $\boldsymbol{\delta} = D\boldsymbol{I}_2$.

The matrix $diag(\boldsymbol{\nu})$ is (naming $diag(\nu_s)$ the rate matrix of the single system):

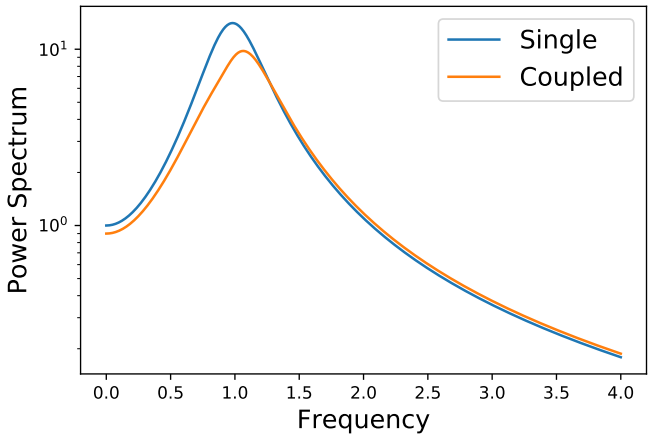

Figure 14: Ressonance factor for the molecular species X (PSD normalitzed by the value at zero) for a single Brusselator (blue) and computed PSD for the coupled double compartment Brusselator (orange). Parameters are $b = 1.5$, $c = 1$ and $K_x = 0.1$, $K_y = 0$.

$$diag(\boldsymbol{\nu}) = \begin{pmatrix} diag(\boldsymbol{\nu}_s) & 0 & \cdots & 0 \\ 0 & diag(\boldsymbol{\nu}_s) & \ddots & \vdots \\ \vdots & \cdots & \boldsymbol{\delta} & 0 \\ 0 & \cdots & 0 & \boldsymbol{\delta} \end{pmatrix} \tag{66}$$

Now, defining $\boldsymbol{\beta} = \boldsymbol{\sigma} \cdot diag(\boldsymbol{\nu}_s) \cdot \boldsymbol{\sigma}^T$, the matrix $\boldsymbol{B} = \boldsymbol{S} \cdot diag(\boldsymbol{\nu}) \cdot \boldsymbol{S}^T$ is computed as

$$\boldsymbol{B} = \begin{pmatrix} \boldsymbol{\beta} + 2\boldsymbol{\delta} & -2\boldsymbol{\delta} \\ -2\boldsymbol{\delta} & \boldsymbol{\beta} + 2\boldsymbol{\delta} \end{pmatrix} \tag{67}$$

Numerical results for coupled compartments

We simulated the Brusselator system in two coupled compartments with parameters $b = 1.8$, $c = 1$ and computed the period distribution for several volumes. The coupling constant was $K = 0.1$ for both X and Y. They are shown in figure 15. In this particular case, the single compartment does better than the coupled ones.

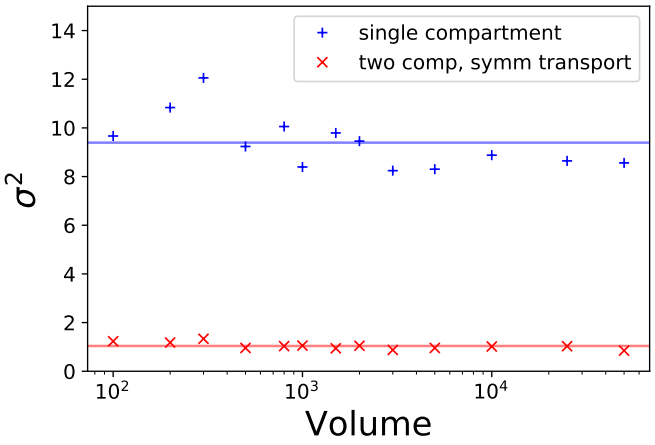

Figure 15: Variance for the periods computed by Gillespie simulations on a Brusselator in the quasicycle regime with $b = 1.8$, $c = 1$. (blue) Single Brusselator (orange) Two coupled Brusselators

Part V
Concluding remarks and further research

The extent of this work has been mostly exploratory. Using the Brusselator as a toy model of a chemical oscillator, we have explored some possible ways of implementing a syncing mechanism that could make a hypothetical biological clock working in a fixed volume more robust to noise. Despite the Brusselator being a very particular case, as well as the configurations that have been explored, we have tried to give some general notions on whether this was possible or not.

In the case of concentration-driven transport between compartments, where the transport term is linear in the concentration difference, we have given an heuristic argument that support the numerical results obtained by stochastic simulation in a computer. In this regard, we have used a phase description of the oscillator. On the one hand, this sort of description hinders establishing a direct relation between this phase picture and the original oscillator as well as correspondence of the coupling functions considered with the original transport terms. On the other hand, this makes for a more general argument, since it gives intuitions on limit-cycle oscillators in general, not just the Brusselator system.

Using this phase-description argument, we established that the gain in robustness due to the synchronization of the two compartments is never greater than the loss by the effective reduction of volumes. Ideally, this two effects cancel each other out, but one has to account for the fluctuations about the mean phase between the two oscillators. This last contribution makes for a slightly less robust oscillator as a whole.

We also implemented an asymmetric transport between compartments, with rates still linear on the concentrations. In this implementation, it was possible for one of the chemical species to change from compartment A to B, but not from B to A. The motivation for this implementation is that, using similar parameters, we observed an improvement in robustness in a similar setup where the transport from A to B was much faster than from B to A. A similar improvement in robustness was observed in the case that we actually showed results of here. In this case, we argue that the dynamical behaviour of the system plays a fundamental role. The asymmetry introduced causes the individual oscillators to function as if some shift in parameters is performed, thus changing the Brusselator on its own, so to speak, and fixating a different robustness coefficient from origin. Whether this is of any biological relevance or not can be an interesting discussion. The parameters b and c used for the Brusselator on this work were arbitrarily chosen, and it just happened that the shift due to the mentioned coupling provided some parameters that appear to be more robust. In this case, it appears more plausible, for the simplicity of the solution, that evolution should fine-tune the parameters to reach some optimum values, rather than developing a more complicated way such as compartmentaliza-

tion, specially since half of the volume used is essentially trashed.

Finally, we also explored the possibility of coupling quasicycle oscillators. The nature of these oscillators is very different from the limit-cycle ones that are more usually considered. Here, noise is not a disrupting agent regarding the oscillations, but rather what fuel them, provided the dynamical picture of the system allows for an amplified frequency to appear. This reflects strongly on the behaviour of the period distribution, since in this case they seem not to depend on the volume of the system. We obtained a formula for the power-spectrum density of the coupled system, up to first order in the coupling coefficients, that should work for small values of the latter. We weren't able to find any regime where the modified PSD had a bigger amplifying coefficient than the original one. However, this may be possible for other parameter regimes or chemical oscillators.

So far, many fundamental questions remain unanswered. Aligning with the results obtained by Gaspard et al. [20] [21] on a genetic model of biological clocks, where cooperation in transcription factors introduced some non-linearities that improved the robustness of the clocks, one could investigate if a non-linear transport term between compartments has a similar effect.

It could also prove interesting to skip the formulation in terms of a chemical oscillator and work with more abstract Kuramoto oscillators, for example. In this way, one should get rid of the specificities of any particular dynamical system and focus on the properties inherent to oscillations on their own. As a comeback, this gets the subject further away from any real implementation in biological systems.

An even more abstract and general question would be: is there an ideal clock? Imagine that one knew all possible biological clocks that could be build in a fixed volume Ω, and then order them by their robustness factors from better to worse. Is there a bound on how good a clock can be, or can it be improved all the way down to being almost deterministic? Which one ends up on the top of the list?

References

[1] Johnson, C.H., Golden, S.S., Ishiura, M. and Kondo, T., 1996, Circadian clocks in prokaryotes, *Molecular Microbiology* 21(1), p. 5-11

[2] The Nobel Assembly at Karolinska Institutet, (2017-10-02), *The Nobel Prize in Pyshiology or Medicine 2017* [Press release]. Retrieved from https://www.nobelprize.org/prizes/medicine/2017/press-release/

[3] Winfree, A.T., 1967, Biological rhythms and the behavior of populations of coupled oscillators, *Journal of Theoretical Biology*, Vol. 16, p.16-42

[4] Dijk, D.J, Czleisler, C.A., 1994, Paradoxical timing of the circadian rhythm of sleep propensity serves to consolidate sleep and wakefulness in humans, *Neuroscience Letters*, Vol. 166, Issue 1, p. 63-68

[5] Antoch M.P. *et al.*, 1997, Functional identification of the mouse circadian Clock gene by transgenic BAC rescue, *Cell*, Vol. 89, Issue 4, p. 655-667

[6] Tsai, T.Y., Choi, Y.S., Ma, W., Pomerening, J.R., Tang, C., Ferrel Jr, J.E., 2008, Robust, tunable biological oscillations from interlinked positive and negative feedback loops, *Science*, Vol. 321, p. 126-129

[7] Kuramoto, Y., 1984, *Chemical Oscillations, Waves and Turbulence*, Springer-Verlag Berlin, Heidelberg, New York, Tokyo, 153 p.

[8] Heltberg, M.L., Krishna, S., Jensen, M.H., 2017, Time Correlations in Mode Hopping of Coupled Oscillators, *Journal of Statistical Physics*, Vol. 167, p. 792-805

[9] Elowitz, M.B., Leibler, S., 2000, A synthetic oscillatory network of transcriptional regulators, *Nature*, Vol. 403, p. 335-338

[10] Strogatz, S.H., 2015, *Nonlinear Dynamics and Chaos*, Westview Press, 2nd Edition

[11] Acebrón, J.A., Bonilla, L.L., Pérez Vicente, C.J., Ritort, F. and Spigler, R., 2005, The Kuramoto model: A simple paradigm for synchronization phenomena, *Reviews of Modern Physics*, Vol. 77, p. 137-185

[12] McKane, A.J., Nagy, J.D., Newman, T.J. and Stefanini, M.O, 2007, Amplified biochemical oscillations in cellular systems, *Journal of Statistical Physics*, Vol. 128, p. 165-191

[13] Boland, R.P., Galla, T., McKane, A.J, 2008, How limit-cycles and quasi-cycles are related in systems with intrinsic noise, *Journal of Statistical Mechanics: Theory and Experiment*, P09001

[14] Barkai, N., Leibler, S., 1997, Robustness in simple biochemical networks, *Nature*, Vol. 387, p. 913-917

[15] Tomita, K. and Tomita, H., 1974, Irreversible Circulation of Fluctuation, *Progress of Theoretical Physics*, Vol. 51, No 6, p. 1731-1749

[16] Nicolis, G., Prigogine, I., 1977, *Self-organization in Nonequilibium Systems*, John Wiley & Sons, USA

[17] Gillespie, D.T., 2000, The chemical Langevin equation, *Journal of Chemical Physics*, Vol. 113, No. 1, p. 297-306

[18] Gillespie, D.T., 1977, Exact stochastic simulation of coupled chemical reactions, *The Journal of Physical Chemistry*, Vol. 81, No. 25, p. 2340-2361

[19] VanKampen, N.G., 2007, *Stochastic Processes in Physics and Chemistry*, Elsevier BV, Amsterdam, Third Edition

[20] Gonze, D., Halloy, J., Gaspard, P., 2002, Biochemical clocks and molecular noise: Theoretical study of robustness factors, *The Journal of Chemical Physics*, Vol. 116, No. 24, p. 10997-11010

[21] Gaspard, P., 2002, The correlation time of mesoscopic chemical clocks, *The Journal of Chemical Physics*, Vol. 117, No. 19, p. 8905-8916

[22] Mitarai, N., Diffusive and Stochastic Processes, *lecture notes*, Niels Bohr Institute (version April 2019)

[23] Pikovsky, A., Rosenblum, M., Kurths, J., 2001, *Synchronization. A universal concept in nonlinear sciences.*, Cambridge University Press

[24] Press, H., Teukolsky, S.A., Vetterling, W.T., Flannery, B.P., 2007, *Numerical Recipes. The Art of Scientific Computing*, Cambridge University Press, Third Edition.